ISSN NO. 2320-5407

Journal homepage: http://www.journalijar.com

INTERNATIONAL JOURNAL OF ADVANCED RESEARCH

RESEARCH ARTICLE

TURBULENT AND INCOMPRESSIBLE FLOW IN A SHELL AND TUBE HEAT EXCHANGER

V. Nagamani[1] and *A. Chennakesava Reddy[2]

1. PG Student, Department of Mechanical Engineering, JNTUH College of Engineering, Hyderabad, India.
2. Professor, Department of Mechanical Engineering, JNTUH College of Engineering, Kukatpally, Hyderabad, Telangana State, India.

Manuscript Info

Manuscript History:

Received: 12 February 2015
Final Accepted: 22 March 2015
Published Online: April 2015

Key words:
Turbulent ,incompressible flow, heat exchanger

Corresponding Author

V. Nagamani

Abstract

The present work is to analyze turbulent and incompressible flow in a cross flow heat exchanger using FLUENT code. The vortex formation length behind the first cylinder is the longest at any time instant. The hotter fluids are confined to the near-wall and wake regions, while a narrow stream of cooler fluid is coveted through the tube bank. The amplitude of the pressure fluctuation increases as the flow develops from the front stagnation point. After the separation point, the pressure fluctuation is approximately kept at the same level. The density is constant.

Copy Right, IJAR, 2015,. All rights reserved

INTRODUCTION

The shell-and-tube heat exchanger is the most versatile type of cross-flow exchangers (Kakac and Liu, 1997) and is the one most widely used in the process and power industries. In the normal configuration, one fluid flows through tubes and second fluid passes around the tubes at 90 degrees angle. Turbulent flow inside the tube bundle depends on the effects of boundary layer separation and interactions of cylinder wakes. In the inline-flow tube bindle, one row of tubes is placed exactly behind the next along the stream-wise direction, without displacement in the cross-flow direction (Ziada and Oengoren, 2000). In staggered arrays, every second row of tubes is displaced resulting in several configurations: symmetric arrays (Balabani, and Yianneskis, 1997), rotated square arrays, normal triangle arrays (Polak, and Weaver, 1995), parallel triangle arrays [5]. All the aforementioned studies are experimental and have revealed very complicated flow features.

Recently, the first direct numerical simulations (DNS) in tube bundle flows have appeared in the literature (Moulinec et al., 2004). The Reynolds number (based on the bulk velocity) is equal to 6000. The computational domain comprises of only an elemental (or periodic) 'cell', assuming fully developed flow in the stream-wise and cross-stream directions. Polak and Weaver (1995) has examined that the vortices shed out from the shear layers in the staggered array are distorted and dissipated by turbulent buffeting in the turbulence generated by the successive downstream tube rows. Free stream turbulence level has a high impact on the flow characteristics inside the inline tube bundle.

Heat exchangers are being used to in many engineering process like those in refrigeration and air Conditioning systems, power systems, food processing system, chemical reactors and space or aeronautical applications. Many engineering systems including engine cooling systems and climate control typically contain turbulent heat exchanger. The objective of the present work was to analyze turbulent and incompressible flow in a

cross flow heat exchanger using FLUENT code. The heat exchanger was made of uniformly spaced staggered tubes arranged in the direction of cross-fluid flow. The fluid was water.

1. Materials and Methods

The staggered tube bundle was equipped with seven horizontal and staggered rows of 22 mm diameter of tubes. The transversal pitch of the tube arrangement was $a = s_t/d = 3$ and the longitudinal pitch of the tube arrangement was $b = s_l/d = 1.8$, wherein, d is the diameter of the tube, s_t is transversal pitch, and s_l is longitudinal pitch. The standard diameter ratios were taken from the Handbook of Heat and Mass Transfer. The staggered tube configuration was similar to that of a shell and tube heat exchanger having cross flow.

In the present work the model was employed the standard k- ε model. The standard k- ε model is a semi-empirical model based on model transport equations for the turbulence kinetic energy (k) and its dissipation rate (ε). In the derivation of the k- ε model, it was assumed that the flow was fully turbulent, and the effects of molecular viscosity were negligible. The standard k- ε model was therefore valid only for fully turbulent flows (Reddy, 2002). The turbulence kinetic energy, k, and its rate of dissipation, ε, were obtained from the following transport equations:

$$\frac{\partial}{\partial t}(\rho k)+\frac{\partial}{\partial t}(\rho k v_i)=\frac{\partial}{\partial x_j}\left[\left(\mu+\frac{\mu_t}{\sigma_k}\right)\frac{\partial k}{\partial x_j}\right]+G_k+G_b-\rho\varepsilon-Y_M+S_k \quad (1)$$

$$\frac{\partial}{\partial t}(\rho k)+\frac{\partial}{\partial t}(\rho k v_i)=\frac{\partial}{\partial x_j}\left[\left(\mu+\frac{\mu_t}{\sigma_\varepsilon}\right)\frac{\partial \varepsilon}{\partial x_j}\right]+C_{1\varepsilon}\frac{\varepsilon}{k}(G_k+C_{3\varepsilon}G_b)-C_{2\varepsilon}\rho\frac{\varepsilon^2}{k}+S_\varepsilon \quad (2)$$

In these equations, G_k represents the generation of turbulence kinetic energy due to the mean velocity gradients, G_b is the generation of turbulence kinetic energy due to buoyancy, Y_M represents the contribution of the fluctuating dilatation in compressible turbulence to the overall dissipation rate. $C_{1\varepsilon}$, $C_{2\varepsilon}$, and $C_{3\varepsilon}$ are constants. σ_k and σ_ε are the turbulent Prandtl numbers for k and ε, respectively. S_k and S_ε are user-defined source terms. The turbulent (or eddy) viscosity, μ, is computed by combining k and ε as follows:

$$\mu_t = \rho C_\mu \frac{k^2}{\varepsilon} \quad (3)$$

where, Cμ is a constant.

The model constants considered in the present work as follows:

$C_{1\varepsilon} = 1.44, C_{2\varepsilon} = 1.92, C_\mu = 0.09, \sigma_k = 1.00, \sigma_k = 1.30$

Shell and tube type heat exchanger of cross flow type was specifically designed for the efficient transfer of heat from one fluid to anther fluid over a solid surface. This transfer of heat could either take the form of absorption or dissipation of heat. The cross flow heat exchanger was modeled as a bank of tubes containing a flowing fluid at one temperature and was immersed in a second fluid in cross-flow at a different temperature. Both fluids were water, and the flow was classified as turbulent and unsteady sate. The mass flow rate of the cross-flow was known, and the model was used to predict the flow and temperature fields that result from convective heat transfer. Due to symmetry of the tube bundle, and the periodicity of the flow inherent in the tube bundle geometry, only a portion of the geometry was modeled in FLUENT, with symmetry applied to the outer boundaries. The resulting mesh was of a periodic module with symmetry. In the present problem, the inflow boundary was defined as a periodic zone, and the outflow boundary defined as its shadow.

Because of the symmetry of tube bank geometry, only a portion of the domain was modeled. The computational domain is shown in figure 1. A mass flow rate of 0.05 kg/s was applied to the inflow boundary of the periodic module. The temperature of the tube wall (T_{wall}) was 400 K and the bulk temperature of the cross-flow water (T_α) was 285 K.

In the present work only two dimensional multi rows of tubes were chosen as the computational domain. The GAMBIT tool was used for geometry modeling and mesh generation (Chennakesava R Alavala, 2008); the FLUENT code is employed for solution and analysis. The fluid properties i.e., pressure, velocity, temperature and density variation of the domain are obtained.

The procedure using GAMBIT was as follows:

1. Creation of the face model.
2. Creation of boundary mesh, edge mesh and face mesh.
1. Specification of the zones.
2. Use of the triangular mesh in 2 for unstructured mesh.
3. Exporting the file to FLUENT Software.

The procedure using FLUENT was as follows:

1. Starting the 2D version of FLUENT.
2. Creating the model geometry and grid.
3. Creating periodic zones.
4. Defining a specified periodic mass flow rate.
5. Modeling periodic heat transfer with specified temperature boundary conditions.
6. Plotting temperature profiles on specified iso-surfaces.
7. Computing and monitoring the solution.
8. Examining and saving the results.

The design adopted for the present work was two-dimensional. Only a portion of the geometry was modeled because of symmetry. The dimensions of rectangle are 75mm x 33mm. The diameter of circle is 22mm. The geometry of domain is shown in figure 2a. Triangular element (Chennakesava R Alavala, 2009) was used to mesh the domain (figure 2b). The following must input to generate mesh:

Height of the first row of mesh elements (1mm)

Total number of rows which defines the depth of the boundary layer (33)

Edge to which the boundary layer was attached

The growth factor was defined as b/a, where, b is the distance between the first and second rows at a given edge node, and a is the height of the first row at the node.

The specify zones were defined as

Inlet	→ periodic
Outlet	→ periodic
Tubes (curved area)	→ wall
Top symmetry	→ symmetry
Bottom symmetry	→ symmetry

The mesh was of 5824 triangular elements, 3053 nodes, 60 faces, 60 symmetry faces, 50 wall faces, 8596 interior faces on the 2D symmetry of the present analysis. Wall-7 and wall-8, the inflow and outflow boundaries, respectively, were defined as wall zones and need to be redefined as periodic. Wall-8 was made into a translational periodic zone, and wall-7 was deleted and redefined as wall-8's periodic shadow.

The 1st-order implicit formulation was sufficient for the present problem. A time-dependent solution was chosen. The time step Δt was restricted to the stability limit of the underlying solver (i.e., a time step corresponding to a Courant number of approximately 1). In order to be time-accurate, all cells in the domain was used the same time step. An incompressible solution was iterated to convergence within each time step. For viscous model the K-epsilon was specified for the turbulent flow. For the periodic flow conditions the mass flow rate was 0.05 kg/s. The water was as the fluid having the following properties:

Density of water	= 998.2 kg/m3,
Specific heat of co-efficient	= 4182 j/kg-k,
Thermal conductivity	= 0.6 w/m-k,
Viscosity	= 0.001003 kg/m-s.

For the 'Operating Conditions' the pressure was set at 101324 pascal. The temperature boundary conditions (400 K) were set for tube 2 (the top wall of the right tube) in the periodic model of the present work. The solution parameters (i.e. flow, turbulence, energy) are as follows:

Under-relaxation factors were changed to the present problem:

Pressure	= 0.3
Density	= 1
Body forces	=1
Momentum forces	= 0.7
Turbulent K.E	= 0.5
Turbulent Dissipation Rate	= 0.7
Discrete Phase Sources	= 0.5

Discretization parameters were set to:

Pressure	= standard
Momentum	= second order upwind
Turbulence kinetic energy	= second order upwind
Turbulence dissipation rate	= second order upwind

3. Results and Discussion

The residuals for convergence criteria are shown in figure 3. The solution convergence shows the effectiveness of the solution assumed for the problem. In the graph it is seen that the convergence criteria leads to converge at 9232 iterations for all. The solution was converged successfully in each variable.

Figure 4a shows the contours of velocity variation from minimum velocity to maximum velocity in fluid flow. The left side vertical bar from bottom to top represents color variation corresponding to velocity values in m/s. The red color indicates the maximum velocity (3.56e-6 m/s) and the blue color indicates the minimum velocity (0). The velocity vectors are displayed in figure 4b. These vectors variation from the low velocity in upper and lower side the curved surface surroundings to maintain the maximum velocity in the middle surface in-between two symmetric walls. The zoomed-in view (figure 4c) of the velocity vector plot clearly shows the re-circulating flow behind the tube and the boundary layer development along the tube surface. The x-axis consists of 'position' of the domain in "mm" y-axis consists of 'velocity magnitude' in m/s as shown in figure 4d. Figure 5 shows the multi rows of tubes indicating the flow of fluids with velocity variation. It displays a list of all symmetry planes in the domain with same periodic inflow and outflow boundary conditions. There are two symmetry zones in the mirror planes i.e. bottom and top symmetry planes in the domain. The vortex formation length behind the first cylinder is the longest at any time instant. The one behind the second cylinder is shorter because the local effective Reynolds number is higher. Figure 6 indicates velocity variation at different iso-surfaces. In this the x-axis consists of "position" of the domain in "mm" y-axis consists of "velocity magnitude" in m/s. for x =-22, 0 & 22, the iso-surfaces corresponding to the vertical cross-sections through the first tube, halfway between the two tubes, and through the second tube. The velocity magnitude is maximum at halfway between the two tubes. The transverse velocity fluctuation follows the stream-wise velocity fluctuation, and both of them are good characteristic lengths for the vortex formation length.

Figure 7a shows the contours of temperature variation in fluid flow. The contours reveal that the temperature increases in the fluid due to heat transfer from the tubes. The hotter fluids are confined to the near-wall and wake regions, while a narrow stream of cooler fluid is coveted through the tube bank. Figure 7b shows the static temperature variation along the fluid flow surface. It can be seen that more cool fluid is recirculated by stronger vortices at the rear of the cylinder. Figure 7c shows the multi rows of tubes indicating the flow of fluids with temperature variation of 285k – 400k. It displays a list of all symmetry planes in the domain with same periodic inflow and outflow boundary conditions. There are two symmetry zones in the mirror planes list i.e. bottom and top symmetry planes in the domain. At most of the time instants, the temperature near the rear stagnation point of the first cylinder is lower than the one near the rear stagnation point of the second cylinder. Figure 7d indicates the static temperature variation at different iso-surfaces. The temperature variation at x =-22.0 and 22. These iso-surfaces corresponding to the vertical cross-sections through the first tube, halfway between the two tubes, and through the second tube. The instantaneous iso-temperature field in the near wake region is then correlated with the turbulent flow field.

Figure 8a shows the contours of pressure variation from minimum velocity to maximum velocity in fluid flow. The minimum pressure range is 0.0038 Pascal and maximum pressure range 0.00476 Pascal. Figure 8b shows the static pressure variation along the fluid flow surface. This is the pressure variation along the fluid flow surface at inlet. Figure 8c shows the static pressure variation along the fluid flow surface at mirror planes. This gives pressure variation at each cross sections x=-22, 0 and 22. These iso-surfaces corresponding to the vertical cross-sections through the first tube, halfway between the two tubes, and through the second tube. The amplitude of the pressure fluctuation increases as the flow develops from the front stagnation point. After the separation point, the pressure fluctuation is approximately kept at the same level.

Figure 8d shows the contours of density are constant across any section. Density (ρ) is 998.0 kg/m^3. Figure 39 shows the density variation along the fluid flow surface at each cross sections: x=-22, 0 & 22. These iso-surfaces corresponding to the vertical cross-sections through the first tube, halfway between the two tubes, and through the second tube. At three iso-surfaces density is constant.

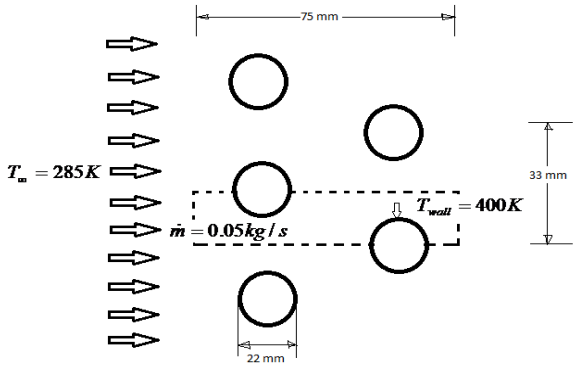

Figure 1: Schematic of shell and tube type heat exchanger

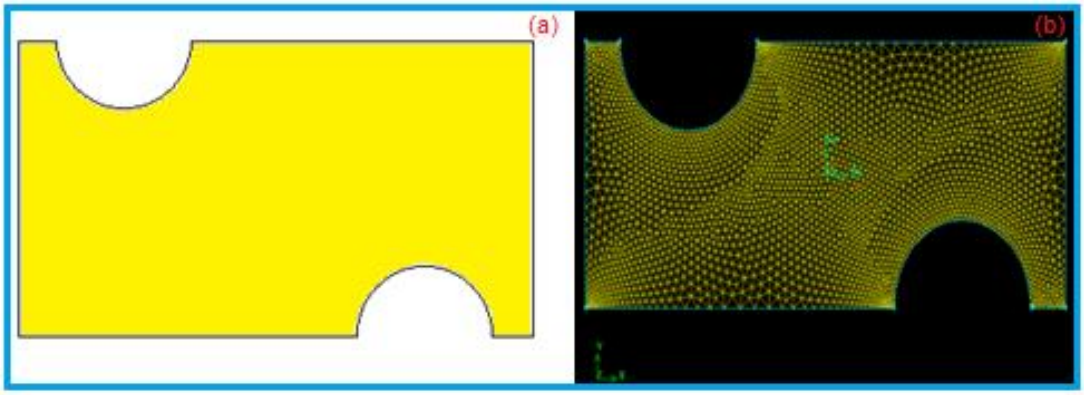

Figure 2: Geometry of the domain (a) and mesh generation for the model (b)

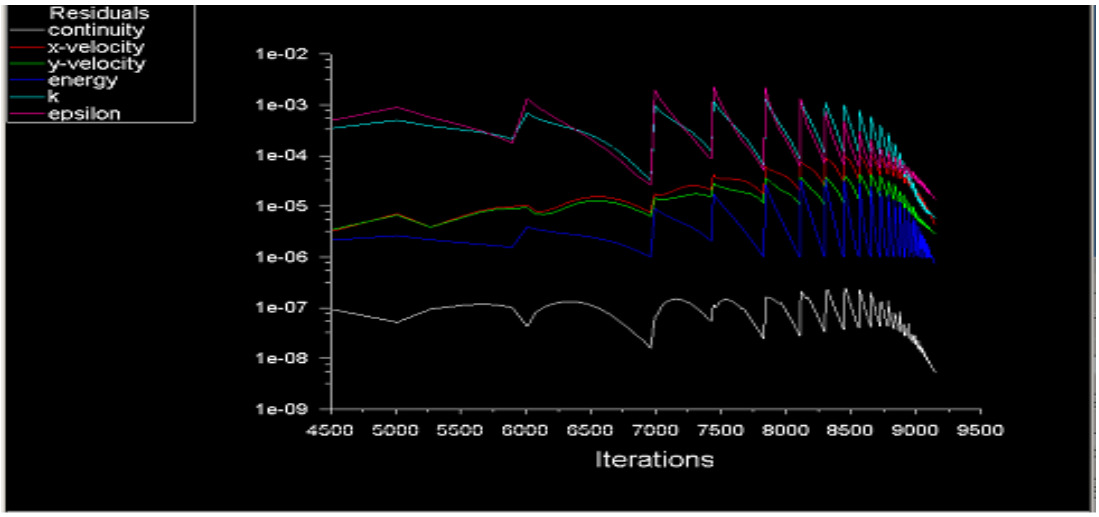

Figure 3: Residuals for convergence criteria

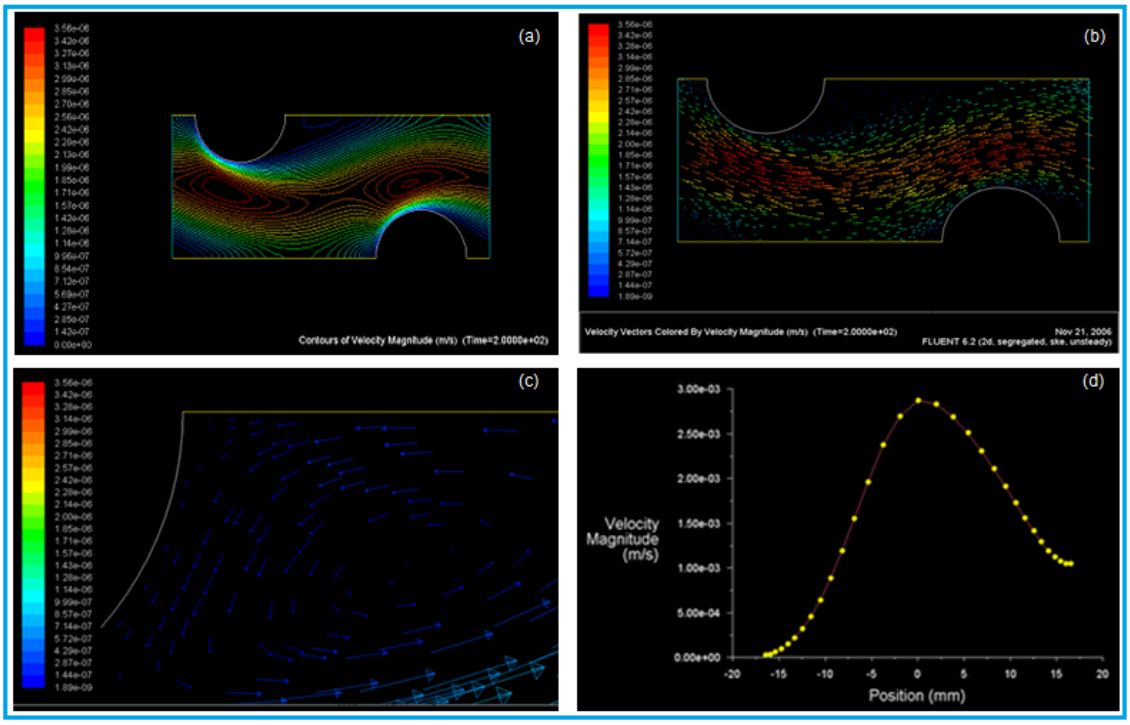

Figure 4: Contours of velocity (a), Zoomed in View of the Velocity Vectors (b), Vectors of velocity (c) and Variation of velocity magnitude along the fluid flow surface (d).

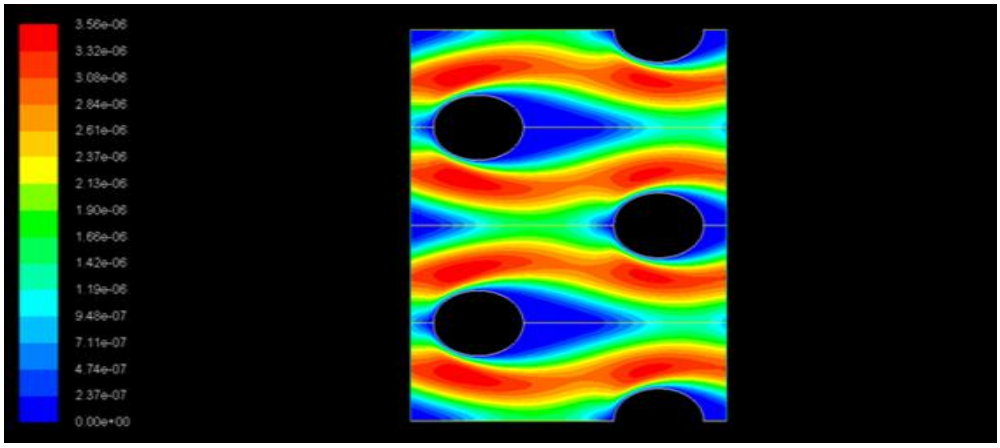

Figure 5: Mirror image of velocity magnitude

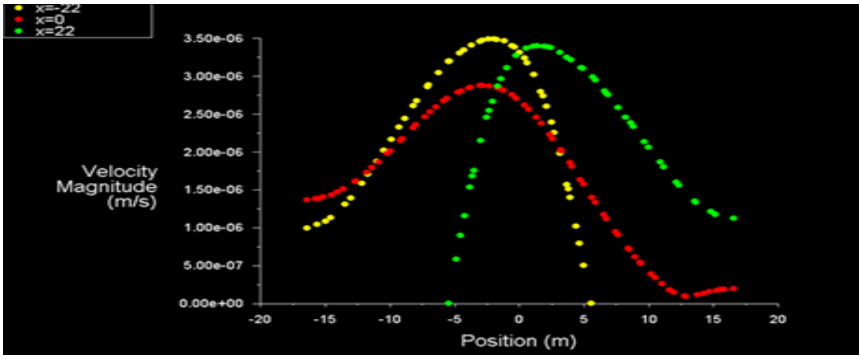

Figure 28: Velocity magnitude at 3 sections

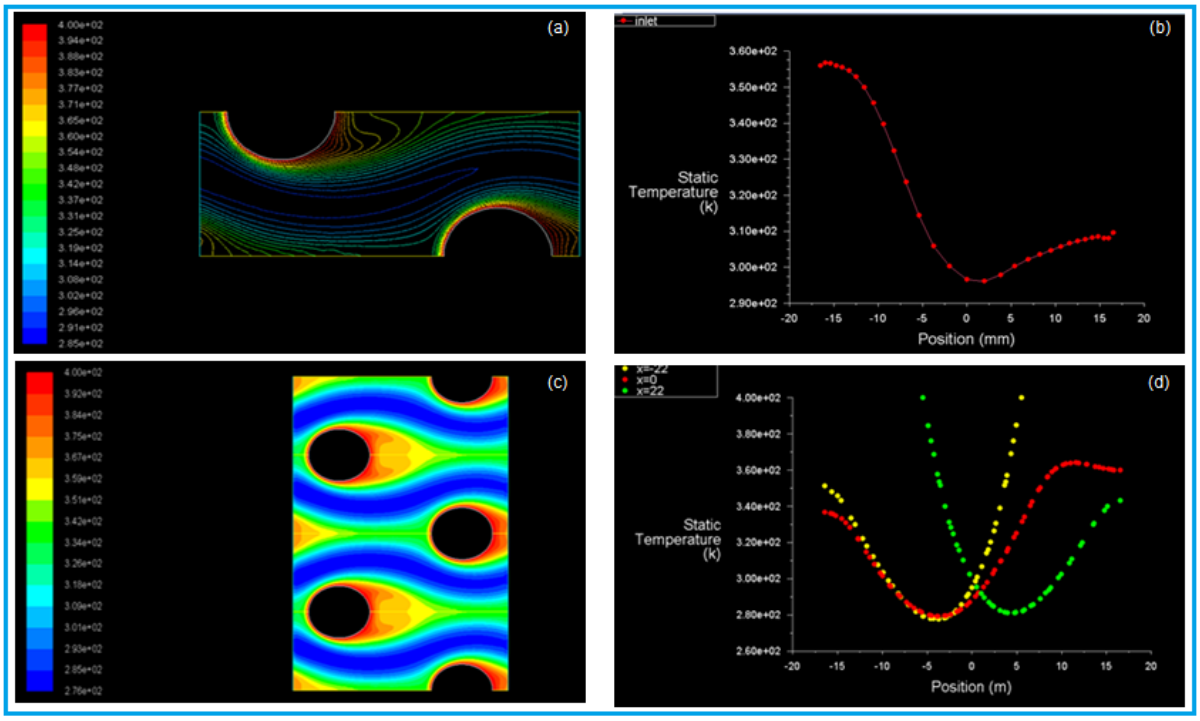

Figure 7: Contours of temperature (a), Static Temperature (b), Mirror image of static temperature (c), and Static temperature at iso-surface (d)

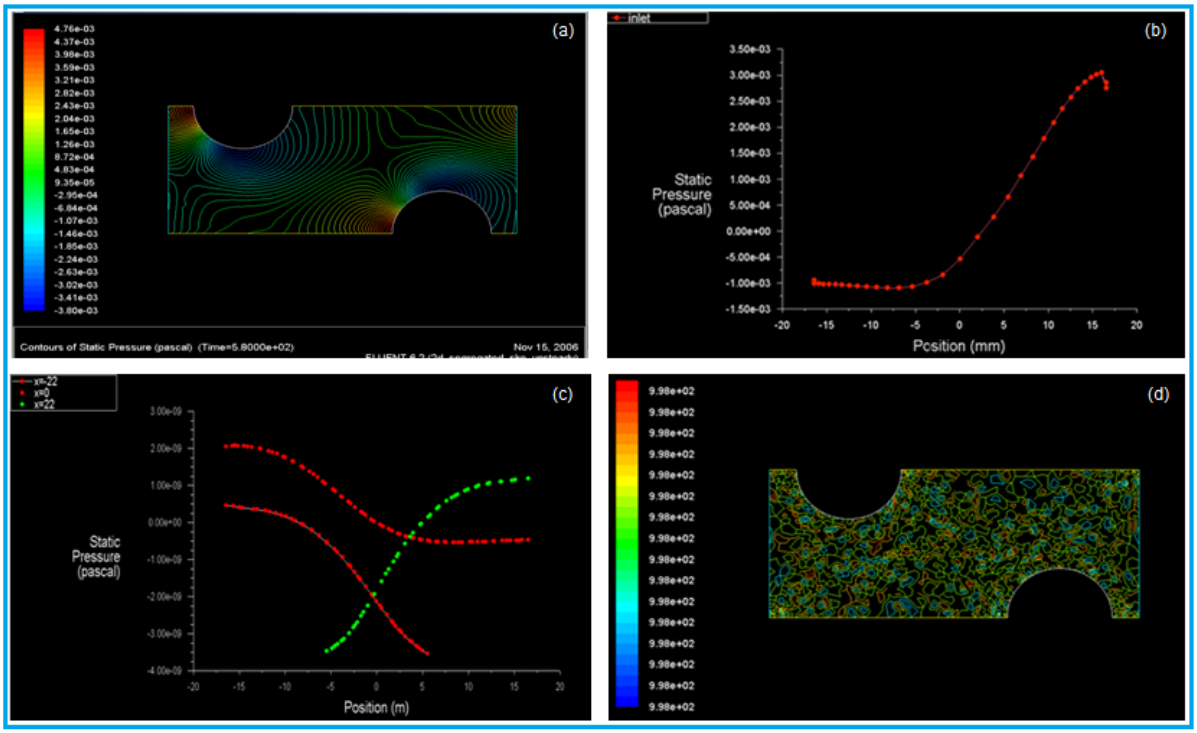

Figure 8: Contours of pressure (a), static pressure (b) static pressure at iso-surface (c) and contours of density (d)

4. CONCLUSIONS

In the present problem, periodic flow and heat transfer in a staggered tube bundle were modeled in FLUENT. The model was set up assuming a known mass flow through the tube bundle and constant wall temperatures. Assuming geometrical model due to the periodic nature of the flow and symmetry of the geometry, only a small piece of the full geometry was modeled. The continuity, momentum and energy equations converged after approximately 9250 iterations when the maximum residual value of $1.0e^{-3}$ was assigned. The fluid flow analysis capabilities could solve unsteady flow patterns for incompressible fluid flow and turbulence enable the prediction of turbulent flow (large changes in velocity over small distances) at the same time in the same model. The tube bundle was specifically designed for the efficient transfer of heat. In this work the capability of computational fluid dynamics analysis for complex heat transfer problems was demonstrated. This experience may lead to improvement of numerical schemes

REFERENCES

and turbulence modeling techniques for industrial complex geometries.

Balabani, S. and Yianneskis, M. (1997). Vortex shedding and turbulence scales in staggered tube bundle flows, Can. J. Chem. Eng., 75 (5):823–831.

Chennakesava Reddy, A. (2002). Computational fluid dynamics analysis of flow over a sine wave shaped wall**,** J. Pumps-N-Valves**,** 2(2):46-47**.**

Chennakesava R Alavala, (2008). CAD/CAM: Concepts and Applications, PHI Learning Pvt. Ltd., New Delhi.

Chennakesava R. Alavala (2009). Finite Element Methods: Basic Concepts and Applications, PHI Learning Pvt. Ltd, New Delhi.

Kakac, S., and Liu, H. (1997). Heat exchangers: selection, rating and thermal design, CRC Press, Boca Raton, FL.

Moulinec, C., Hunt, J.C.R., and Nieuwstadt, F.T.M. (2004). Disappearing wakes and dispersion in numerically simulated flows through tube bundles, Flow Turbul. Combust., 73:95–116.

Polak, D.R. and Weaver, D.S. (1995). Vortex shedding in normal triangular tube arrays, J. Fluid Struct., 9:1–17.

Price, J.S., Paidoussis, M.P., and Mark, B. (1995). Flow visualization of the interstitial cross-flow through parallel triangular and rotated square arrays of cylinders, J. Sound Vib., 181:85–98.

Ziada, S. and Oengoren, A. (2000). Flow periodicity and acoustic resonance in parallel triangle tube bundles, J. Fluid and Struct., 14:197–219.